Detection and Estimation of Icing in Unmanned Aerial Vehicles using a Bank of Unknown Input Observers

Maria M. Seron[1] Tor A. Johansen[2*] José A. De Doná[1] Andrea Cristofaro[2]

Abstract— **Icing is regarded as a severe structural alteration affecting unmanned aerial vehicles (UAVs), since ice accretion on wings and control surfaces modifies the aircraft shape resulting in altered controllability and performance of the vehicle. We study the problem of detection of icing and estimation of its 'severity' factor in longitudinal control of UAVs. We propose to employ a bank of unknown input observers (UIOs), each designed to match a model of the aircraft under a particular level of icing taken from a quantisation of the icing's severity factor range of variation. The UIO design exploits the change in equilibrium conditions, caused by the icing effect, to identify a direction in the observer estimation error space that allows for aircraft icing detection and estimation. By selecting at each time the observer from the bank that yields the smallest value of a suitable residual signal, the icing severity factor can be estimated with an accuracy that is inversely proportional to the size of the quantisation level.**

I. Introduction

Structural faults in dynamical systems lead to changes in the nominal system dynamics. The problem of correct estimation of the fault characteristics is critical for the application of accommodation policies that aim at ensuring safe operational conditions and, if possible, recovering certain levels of system performance.

Icing is regarded as a major structural fault in unmanned aerial vehicles (UAVs). The phenomenon of ice accretion on aircraft wings and control surfaces is a well recognised problem in aerospace systems: when ice layers build up, they increase energy consumption and induce a safety risk, with the worst case scenario that the aircraft crashes [7]. Large airplanes are commonly equipped with efficient anti-icing and de-icing devices; however, these are mostly unsuitable for small aircrafts, due to their simple architecture and limited payload. Recently, some advanced de-icing devices for UAVs have been proposed based on carbon nanotubes technology [2]. The wing surface can be painted with layers of coating material, which can be heated up very quickly using electricity. However, the efficiency of this mechanism strongly relies on icing detection and estimation schemes with fast and accurate responses.

Several approaches have been proposed for icing detection in aircrafts and UAVs, including fault detection and diagnosis methods [10], [14], [13] and Kalman filtering [3]. An unknown input observer (UIO) based approach for icing detection in UAVs was used in [5], where a design scheme for detection filters able to decouple icing effects from actuators or sensor faults was proposed. In [6], a multiple-model adaptive estimator is proposed for icing detection and identification in small UAVs. Defining a bank of possible models corresponding to distinct admissible values of the icing factor, the proposed algorithm guarantees the identification of the closest model to the true system as well as the estimation of the icing severity factor.

In this paper we combine the UIO and multiple-model approaches to propose a scheme that has the double advantage of having a simpler structure while allowing the estimation of the icing's severity factor with prespecified accuracy. We first analyse stability of the closed-loop system trajectories under icing using linear parameter varying (LPV) techniques. In addition, we study the changes caused by icing on the equilibrium values of the system variables and exploit these changes in the UIO design. Specifically, offsets produced by icing on certain variables can be used to define directions in the observer estimation error space, which can be associated with icing detection and estimation of its severity factor. In addition, the UIO design decouples the icing effect from the wind disturbances, the latter associated with different directions in the estimation error space. We propose to employ a bank of UIOs, each designed to match a model of the aircraft under a particular level of icing taken from a quantisation of the icing's severity factor range of variation. By selecting at each time the observer from the bank that yields the smallest value of a suitable residual signal, we show that the icing's severity factor can be estimated with an accuracy that depends on the size of the quantisation level. Simulation results show the efficiency of the proposed estimation algorithm.

II. UAV Longitudinal Motion Model

The longitudinal equations of motion of an unmanned aerial vehicle (UAV), linearised about an operating point, have the form [1], [5]

$$\dot{x} = Ax + Bu + H_x v^x + H_z v^z, \qquad y = Cx, \qquad (1)$$

where the state $x = (\nu, w, q, \theta)$, represents deviation variables with respect to the operating point $x^* = (\nu^*, w^*, q^*, \theta^*)$, and consists of (deviation values of) horizontal airspeed, ν, vertical airspeed, w, pitch rate, q, and pitch angle, θ; the control input $u = (\delta_{th}, \delta_e)$ consists of (deviation values with respect to the corresponding input

* This work is partly sponsored by the Research Council of Norway by the KMB project D2V, project number 210670, and through the Centres of Excellence funding scheme, grant number 223254 – AMOS.

[1] Priority Research Centre for Complex Dynamic Systems and Control School of Electrical Engineering and Computer Science The University of Newcastle, Australia, maria.seron, jose.dedona@newcastle.edu.au

[2] Department of Engineering Cybernetics, Norwegian University of Science and Technology and Center for Autonomous Marine Operations and Systems (AMOS), Norway, tor.arne.johansen@itk.ntnu.no

operating point, $u^* = (\delta_{th}^*, \delta_e^*)$, of) engine throttle δ_{th} and elevator deflection δ_e; the disturbance (v^x, v^z) consists of the wind acceleration in the horizontal and vertical directions, respectively. Assuming that the UAV is equipped with an airspeed measurement device (pitot tube), GPS and inertial sensors, all state variables can be measured or estimated [1] and hence in the output equation we consider $C = I$.

The matrices in (1) have the form

$$A = \begin{bmatrix} X_\nu & X_w & X_q & -g\cos\theta^* \\ Z_\nu & Z_w & Z_q & -g\sin\theta^* \\ M_\nu & M_w & M_q & 0 \\ 0 & 0 & 1 & 0 \end{bmatrix}, \tag{2}$$

$$B = \begin{bmatrix} X_{th} & X_e \\ 0 & Z_e \\ M_{th} & M_e \\ 0 & 0 \end{bmatrix},\ H_x = \begin{bmatrix} -\cos\theta^* \\ -\sin\theta^* \\ 0 \\ 0 \end{bmatrix},\ H_z = \begin{bmatrix} -\sin\theta^* \\ \cos\theta^* \\ 0 \\ 0 \end{bmatrix}, \tag{3}$$

where g is the gravity acceleration constant. The coefficients X_i, Z_i and M_i, $i \in \{\nu, w, q, th, e\}$, in the above matrices are functions of the operating point and the aircraft aerodynamic parameters see, e.g., [1, Chapter 5, p. 86].

For the above model we will consider a state feedback control with integral action, of the form

$$u = Kx + \bar{K}s, \quad \dot{s} = \bar{C}x, \tag{4}$$

where s is the integral action state and $[K\ \bar{K}]$ are designed such that $\begin{bmatrix} A+BK & B\bar{K} \\ \bar{C} & 0 \end{bmatrix}$ is Hurwitz. The matrix

$$\bar{C} \triangleq \begin{bmatrix} 1 & 0 & 0 & 0 \\ 0 & 1 & 0 & 0 \end{bmatrix} \tag{5}$$

selects the horizontal airspeed and vertical airspeed as the state components for which it is desired to preserve the equilibrium values in the presence of constant disturbances, including moderate levels of icing.

III. Icing Effect Model

The effect of icing accumulation on the aircraft surfaces produces structural changes in the system which can be modelled on the linearised deviation equations as follows [5]:

$$\dot{x} = Ax + Bu + H_x v^x + H_z v^z + \mathcal{E}(x,u)\eta, \tag{6}$$

where

$$\mathcal{E}(x,u) \triangleq A_{\text{ice}}x + B_{\text{ice}}u + F_{\text{ice}}, \tag{7}$$

is the aircraft icing distribution vector and η is the aircraft surface icing severity factor (typically considered as bounded between 0, corresponding to the 'clean' condition and 0.2, corresponding to the 'all-iced' condition). The matrices in (7) are given by

$$A_{\text{ice}} = \begin{bmatrix} \mathcal{E}_{X_\nu} & \mathcal{E}_{X_w} & \mathcal{E}_{X_q} & 0 \\ \mathcal{E}_{Z_\nu} & \mathcal{E}_{Z_w} & \mathcal{E}_{Z_q} & 0 \\ \mathcal{E}_{M_\nu} & \mathcal{E}_{M_w} & \mathcal{E}_{M_q} & 0 \\ 0 & 0 & 0 & 0 \end{bmatrix},\ B_{\text{ice}} = \begin{bmatrix} 0 & \mathcal{E}_{X_e} \\ 0 & \mathcal{E}_{Z_e} \\ 0 & \mathcal{E}_{M_e} \\ 0 & 0 \end{bmatrix}, \tag{8}$$

where the coefficients depend on the aircraft specifications [11]; and F_{ice} is an offset caused by a shift in the equilibrium point due to the icing effect on force balances.

Using (4), the aircraft icing distribution vector $\mathcal{E}(x,u)$ in (7) can be expressed as

$$\mathcal{E}(x,u) = (A_{\text{ice}} + B_{\text{ice}}K)x + B_{\text{ice}}\bar{K}s + F_{\text{ice}}. \tag{9}$$

For a fixed value of the icing severity factor η, the offset term in the above equation, F_{ice}, causes a change in the equilibrium point of the deviation system. By design, the integral action control restores the equilibrium values for horizontal and vertical airspeeds; however, the pitch angle cannot be compensated by the integral action and will change its equilibrium value.[1] This change in the equilibrium conditions is analysed in the following section considering 'quasi steady-state' values of the system variables under slow variations of the icing severity factor. The equilibrium value changes will be key to making the UIOs sensitive to the effect of icing for its detection and estimation, as explained in Section V.

IV. Closed-loop Stability and Quasi Steady-state Analysis

The closed-loop dynamic equations are obtained using (6), (4) and (9) as

$$\begin{bmatrix} \dot{x} \\ \dot{s} \end{bmatrix} = \underbrace{\begin{bmatrix} (A+BK) + (A_{\text{ice}} + B_{\text{ice}}K)\eta & (B + B_{\text{ice}}\eta)\bar{K} \\ \bar{C} & 0 \end{bmatrix}}_{\mathcal{A}(\eta)} \begin{bmatrix} x \\ s \end{bmatrix} + \underbrace{\begin{bmatrix} H_x \\ 0 \end{bmatrix}}_{\bar{H}_x} v^x + \underbrace{\begin{bmatrix} H_z \\ 0 \end{bmatrix}}_{\bar{H}_z} v^z + \underbrace{\begin{bmatrix} F_{\text{ice}} \\ 0 \end{bmatrix}}_{\bar{F}_{\text{ice}}} \eta. \tag{10}$$

Since the icing coefficient η is generally time-varying but bounded, and the wind disturbances can be assumed bounded, the above system can be regarded as an LPV system with bounded parameter variation and bounded perturbations. We next use results from [8] to establish ultimate boundedness for the dynamics (10). First, we formally state an assumption on the perturbation bounds. In the remainder of the paper, the bars $|\cdot|$ denote elementwise magnitude (absolute value) and the inequalities and max operations are interpreted elementwise.

Assumption IV.1 *The icing coefficient satisfy $\eta \in [0, \varepsilon]$ and the wind acceleration disturbances are bounded as $|v^x| \leq \overline{v^x}$, $|v^z| \leq \overline{v^z}$, for known positive constants ε, $\overline{v^x}$ and $\overline{v^z}$.* ∘

[1] In practice, an altitude controller in a loop outside the controller (4) will adjust the setpoint for pitch after icing occurs in order to compensate for the loss of lift caused by icing. Here we do not consider this outer loop and, instead, focus on the icing detection and estimation mechanism without pitch compensation. The analysis of the effect of icing under the overall controller, including the outer loop, and its implications for icing detection and estimation, will be the subject of future research.

Proposition IV.2 *Consider system* (10) *under Assumption IV.1. Suppose an invertible (possibly complex) transformation V exists such that the matrix*[2]

$$\Lambda \triangleq \max_{\eta\in\{0,\varepsilon\}} \mathcal{M}(V^{-1}\mathcal{A}(\eta)V) \tag{11}$$

is Hurwitz. Then, letting $z \triangleq \begin{bmatrix} x^T & s^T \end{bmatrix}^T$, the set

$$\mathcal{Z} \triangleq \{z : |V^{-1}z| \le b\}, \tag{12}$$

where $b \triangleq (-\Lambda^{-1})\big[|V^{-1}\bar{H}_x|\overline{v^x}+|V^{-1}\bar{H}_z|\overline{v^z}+|V^{-1}\bar{F}_{\rm ice}|\varepsilon\big]$, is invariant for system (10) *and such that its trajectories ultimately converge to the set for any initial condition.*

Proof: It follows by direct adaptation, to the LPV case, of the results of [8] for switched linear systems. ■

Remark IV.3 *The transformation V required in Proposition IV.2 can be searched numerically; for example, an algorithm is presented in [8]. A simpler, possibly more conservative, method that works in some cases (see the example in Section VII) is to take V as the matrix that transforms $\mathcal{A}(\eta)$, for some admissible value of η, to its Jordan canonical form, and then check that the resulting matrix Λ in* (11) *is Hurwitz.* ○

Assuming slow variations of the icing coefficient η, we can study the quasi steady-state solution of the above equations for $\eta \approx \bar{\eta}$ constant in the absence of wind disturbances. Let $\bar{x} = (\bar{\nu}, \bar{w}, \bar{q}, \bar{\theta})$ and $\bar{s}$ be the quasi steady-state values satisfying $\dot{\bar{x}} \approx 0$ and $\dot{\bar{s}} \approx 0$. The integral action (4), (5) implies $0 \approx \bar{C}\bar{x} = (\bar{\nu}, \bar{w})$ and hence

$$\bar{x} = (0, 0, 0, \bar{\theta}), \tag{13}$$

(where we have also used $\bar{q} = 0$, which follows from the form of the matrices in (2), (8)). Then, setting $\dot{x} = 0$ and $\eta = \bar{\eta}$ in the x equation in (10), evaluated at the quasi steady-state values $x = \bar{x}$ from (13) and $s = \bar{s}$, and for zero wind disturbances, yields[3]

$$\begin{aligned} 0 = \big[(A+BK) + (A_{\rm ice}+B_{\rm ice}K)\bar{\eta}\big]\Big|_{(:,4)}\bar{\theta} \\ + (B\bar{K} + B_{\rm ice}\bar{K}\bar{\eta})\,\bar{s} + F_{\rm ice}\bar{\eta} \end{aligned} \tag{14}$$

Define the matrices

$$\Psi \triangleq \begin{bmatrix} (A+BK)\big|_{(:,4)} & B\bar{K} \end{bmatrix}, \tag{15}$$

$$\Phi \triangleq \begin{bmatrix} (A_{\rm ice}+B_{\rm ice}K)\big|_{(:,4)} & B_{\rm ice}\bar{K} \end{bmatrix}. \tag{16}$$

Then, (14) can be rewritten as

$$0 = \Psi \begin{bmatrix} \bar{\theta} \\ \bar{s} \end{bmatrix} + \Phi\,\bar{\eta} \begin{bmatrix} \bar{\theta} \\ \bar{s} \end{bmatrix} + F_{\rm ice}\bar{\eta}, \tag{17}$$

from which

$$\begin{bmatrix} \bar{\theta} \\ \bar{s} \end{bmatrix} = -(\Psi + \Phi\,\bar{\eta})^{\dagger} F_{\rm ice}\,\bar{\eta}, \tag{18}$$

where † denotes the Moore-Penrose pseudoinverse.[4]

Letting $x_{[1:3]} = (\nu, w, q)$ and $\Gamma \triangleq (A_{\rm ice}+B_{\rm ice}K)\big|_{(:,[1:3])}$, we will use the above quasi-steady state values to approximate the icing distribution vector (9) as

$$\begin{aligned} \mathcal{E}(x,u) &= \Gamma x_{[1:3]} + \Phi \begin{bmatrix} \theta \\ s \end{bmatrix} + F_{\rm ice} \\ &\approx \Gamma x_{[1:3]} + \Phi \begin{bmatrix} \bar{\theta} \\ \bar{s} \end{bmatrix} + F_{\rm ice} \\ &= \Gamma x_{[1:3]} + [I - \Phi\,\bar{\eta}(\Psi + \Phi\,\bar{\eta})^{\dagger}]F_{\rm ice}. \end{aligned} \tag{19}$$

V. UIO for Icing Detection and Estimation

Unknown input observers [4] employ the available known signals to construct an estimate of the system state so that the estimation error satisfies certain desirable properties. For example, different components of the estimation error can be made to reflect the action of different unknown input signals provided they affect the system dynamics in different directions. In this work we propose a design that makes the state estimation error components sensitive to the icing severity factor and the wind disturbances.

The observer dynamic equations are given by

$$\begin{aligned} \dot{z} &= Fz + RBu + Sy, \\ \hat{x} &= z + Ty, \end{aligned} \tag{20}$$

where the matrices satisfy

$$\begin{aligned} &S = S_a + S_b, \\ &R = I - TC, \\ &F = RA - S_aC = -\mathrm{diag}\{\lambda_1, \ldots, \lambda_n\}, \quad \lambda_j > 0, \\ &S_b = FT. \end{aligned} \tag{21}$$

It can be shown by direct calculation, using (6) and (20)–(21), that the state estimation error $\tilde{x} \triangleq x - \hat{x}$ satisfies

$$\dot{\tilde{x}} = F\tilde{x} + R[\mathcal{E}(x,u)\,\eta + H_x v^x + H_z v^z], \tag{22}$$

and further using (19)

$$\begin{aligned} \dot{\tilde{x}} = F\tilde{x} + R[I - \Phi\,\bar{\eta}(\Psi + \Phi\,\bar{\eta})^{\dagger}]F_{\rm ice}\eta \\ + R\Gamma x_{[1:3]}\eta + R(H_x v^x + H_z v^z). \end{aligned} \tag{23}$$

Assumption V.1 *The (4×3) matrix*

$$B_A \triangleq \big[[I - \Phi\,\bar{\eta}(\Psi + \Phi\,\bar{\eta})^{\dagger}]F_{\rm ice} \quad H_x \quad H_z\big] \tag{24}$$

has full column rank. ○

Following [5], the matrix R can be designed so that

$$R\,B_A = \begin{bmatrix} I_3 \\ 0 \end{bmatrix} \tag{25}$$

[2]The '*Metzler*' operator $\mathcal{M}(\cdot)$ is defined as follows: $M = \mathcal{M}(N)$ has entries $M_{i,j} = \mathrm{Re}\{N_{i,j}\}$ if $i = j$ and $M_{i,j} = |N_{i,j}|$ if $i \neq j$.

[3]We use $M\big|_{(:,i)}$ to denote the ith column of the matrix M and $M\big|_{(:,[i:j])}$ to denote the submatrix of M formed by columns i to j.

[4]Note that, from the form of the system matrices in (2), (8), the 4×3 matrix $(\Psi + \Phi\,\bar{\eta})$ has the last row equal to zero, hence the pseudoinverse is actually the inverse, provided it exists, of the submatrix formed by the first 3 rows. If the inverse does not exist, then an equilibrium point can still be computed from (17).

and, hence,

$$\dot{\tilde{x}} = F\tilde{x} + \begin{bmatrix} \eta \\ v^x \\ v^z \\ 0 \end{bmatrix} + R\,\Gamma x_{[1:3]}\eta. \tag{26}$$

Modulo transient responses, the first three estimation error components directly respond to aircraft icing and horizontal and vertical wind acceleration disturbances, respectively. The last term in (26), however, although bounded, can potentially lead to large errors in the detection and estimation of the icing coefficient. In addition, the use of the quasi steady-state approximation (19) will introduce errors in the estimation of values of η not close enough to $\bar{\eta}$ (see the top plot in Figure 2, where η varies between 0 and 0.14 and $\bar{\eta} = 0.1$). Thus, in the following section we propose a multiple UIOs scheme that reduces the error in the estimation of the aircraft icing severity factor inversely proportionally to the number of observers.

VI. Bank of 'Icing-Corrected' UIOs

We consider a bank of UIOs with correction terms that are aimed at compensating for icing with some factor $\bar{\eta}_i \in [0, \varepsilon]$. After gridding the interval $[0, \varepsilon]$ each UIO in the bank is designed for a value of $\bar{\eta}_i$ in the grid, that is, we let $\bar{\eta}_i = i\varepsilon/N$, for $i = 0, \ldots, N$, with $N > 1$ equal to the number of subintervals in the grid. The correction term in each UIO takes the following form, using an estimate of the icing effect:

$$\mathcal{E}(x, u)\bar{\eta}_i = (A_{\text{ice}}x + B_{\text{ice}}u + F_{\text{ice}})\bar{\eta}_i. \tag{27}$$

The icing-corrected UIO dynamics are then (cf. (20))

$$\begin{aligned} \dot{z}_i &= F_i z_i + R_i(Bu + \mathcal{E}(x, u)\bar{\eta}_i) + S_i y, \\ \hat{x}_i &= z_i + T_i y, \end{aligned} \tag{28}$$

and the dynamics of the associated state estimation error $\tilde{x}_i \triangleq x - \hat{x}_i$ take the form (cf. (23))

$$\begin{aligned} \dot{\tilde{x}}_i = F_i\tilde{x}_i &+ R_i[I - \Phi\,\bar{\eta}_i(\Psi + \Phi\,\bar{\eta}_i)^\dagger]F_{\text{ice}}(\eta - \bar{\eta}_i) \\ &+ R_i\Gamma x_{[1:3]}(\eta - \bar{\eta}_i) + R_i(H_x v^x + H_z v^z). \end{aligned} \tag{29}$$

Designing the matrix R_i so that

$$R_i\big[[I - \Phi\,\bar{\eta}_i(\Psi + \Phi\,\bar{\eta}_i)^\dagger]F_{\text{ice}} \quad H_x \quad H_z\big] = \begin{bmatrix} I_3 \\ 0 \end{bmatrix} \tag{30}$$

and letting F_i, R_i, S_i and T_i satisfy the corresponding equations (21), yields

$$\dot{\tilde{x}}_i = F_i\tilde{x}_i + \begin{bmatrix} \eta - \bar{\eta}_i \\ v^x \\ v^z \end{bmatrix} + R_i\Gamma x_{[1:3]}(\eta - \bar{\eta}_i). \tag{31}$$

Denote by $\tilde{x}_{i,1}$ the first component of $\tilde{x}_i$ and let $e_1^T = (1, 0, \ldots, 0)$. Then, from (31),

$$\dot{\tilde{x}}_{i,1} = -\lambda_{i,1}\,\tilde{x}_{i,1} + (\eta - \bar{\eta}_i)[1 + e_1^T R_i\Gamma x_{[1:3]}]. \tag{32}$$

Note that $x_{[1:3]}$ moves around zero (due to the integral action) with—typically fast—variations caused by the wind disturbances. If η varies slowly and $\lambda_{i,1}$ is small enough, then the above first order system aproximately yields

$$\tilde{x}_{i,1} \approx (\eta - \bar{\eta}_i)/\lambda_{i,1}. \tag{33}$$

Thus, the UIO in the bank that has its corresponding value of $\bar{\eta}_i$ "closest" to the current value of η will yield the smallest value of its first component (weighed by $\lambda_{i,1}$) when compared with the weighed first component of the other UIOs. This motivates the following aircraft icing estimation algorithm.

Algorithm VI.1 (Aircraft icing estimation) *Consider a bank of $N > 1$ UIOs of the form* (28)*, with $\bar{\eta}_i = i\varepsilon/N$, for $i = 0, \ldots, N$, with its matrices computed using* (25) *and the corresponding equations* (21)*. At each time, compute the current estimate $\hat{\eta}$ of η as*

$$\hat{\eta} = \lambda_{\ell,1}\,\tilde{x}_{\ell,1} + \bar{\eta}_\ell, \quad \ell = \arg\min_{i=1,\ldots,N} |\lambda_{i,1}\,\tilde{x}_{i,1}|, \tag{34}$$

where $\tilde{x}_{i,1}$ is the first component of each UIO's output estimation error $\tilde{x}_i = x - \hat{x}_i$. ∘

The performance of Algorithm VI.1 is illustrated in the case study of the following section.

VII. Case Study

We consider the case study of a small unmanned aircraft, the Aerosonde UAV (AAI Corporation, Textron Inc., see [1], [5]). Taking the operating point $x^* = (\nu^*, w^*, q^*, \theta^*) = (22.96, 2.54, 0, 0.11)$, $u^* = (\delta_{th}^*, \delta_e^*) = (0.34, -0.13)$, and the system parameters as in [5], [1] yields the system matrices

$$A = \begin{bmatrix} -0.4922 & -0.2345 & -2.5376 & -9.7407 \\ -0.6122 & -2.1388 & 22.9578 & -1.0767 \\ 0.0563 & -0.5092 & -0.4609 & 0 \\ 0 & 0 & 1 & 0 \end{bmatrix},$$

$$B = \begin{bmatrix} 41.3783 & 0 \\ 0 & 4.9616 \\ 0 & -15.5684 \\ 0 & 0 \end{bmatrix}, \; H_x = \begin{bmatrix} -0.9939 \\ -0.1099 \\ 0 \\ 0 \end{bmatrix}, \; H_z = \begin{bmatrix} -0.1099 \\ 0.9939 \\ 0 \\ 0 \end{bmatrix}.$$

The feedback gains K and $\bar{K}$ in (4) is designed via LQR with weights $Q_{LQR} = \text{diag}\{0.3, 10, 10, 50, 2, 2\}$ and $R_{LQR} = \text{diag}\{20, 10\}$. This yields

$$K = \begin{bmatrix} -0.1631 & 0.1015 & 0.0822 & -1.3845 \\ -0.0375 & 0.4000 & 1.9919 & 9.4438 \end{bmatrix}, \; \bar{K} = \begin{bmatrix} -0.2772 & 0.1522 \\ -0.2152 & -0.3920 \end{bmatrix}.$$

The matrices in the icing distribution vector (7) are given by

$$A_{\text{ice}} = \begin{bmatrix} -0.0890 & -0.0098 & 0 & 0 \\ 0.1387 & 1.0509 & 0 & 0 \\ -0.0597 & 0.2490 & 0.0809 & 0 \\ 0 & 0 & 0 & 0 \end{bmatrix},$$

$$B_{\text{ice}} = \begin{bmatrix} 0 & 0 \\ 0 & -2.3667 \\ 0 & 7.7842 \\ 0 & 0 \end{bmatrix}, \quad F_{\text{ice}} = \begin{bmatrix} -1.0337 \\ 2.9259 \\ -0.3692 \\ 0 \end{bmatrix}.$$

For the above data and $\eta \in [0, 0.2]$ the stability condition in Proposition IV.2 holds, that is, the matrix (11), computed with V as discussed in Remark IV.3, is Hurwitz, and hence the closed-loop trajectories remain ultimately bounded in the presence of ice.

For the simulation, the horizontal and vertical components of the wind disturbances are generated by a Dryden model (see, e.g., [9]) with parameters as given in [12]. We consider a profile for the icing severity factor η as shown by the

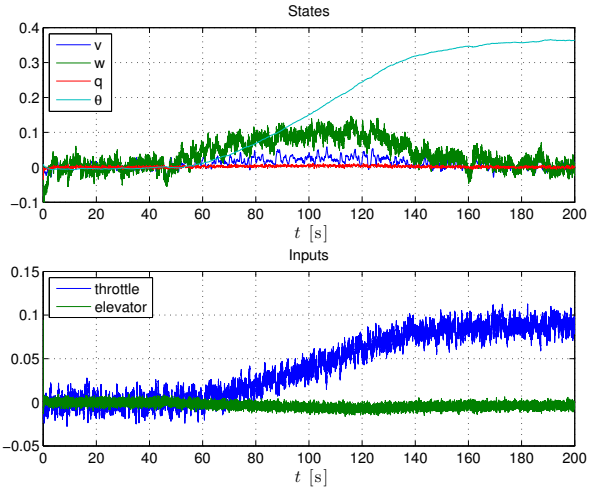

Fig. 1. State and input trajectories under icing.

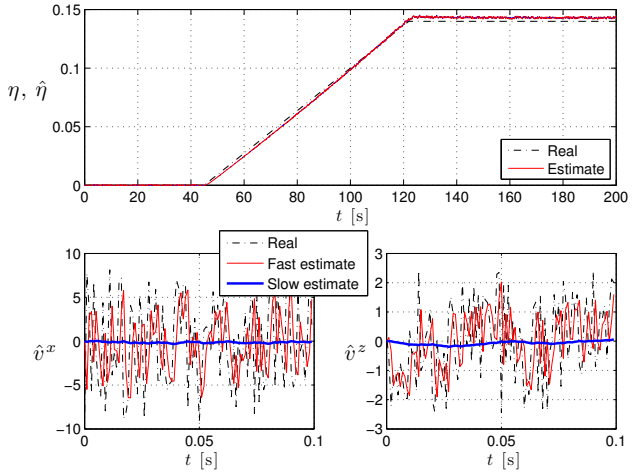

Fig. 2. Estimation of η (top) and wind disturbance components (bottom) with a single UIO.

dashed line in the top plot of Figure 2, starting from 0 at t=45s and evolving linearly until it reaches a maximum value of 0.14 at t=122s. The responses of the closed-loop system (deviation) states and inputs are shown in Figure 1. We can see that, due to the integral action, the horizontal and vertical airspeeds are restored to its equilibrium values around zero whereas the pitch angle trajectory shifts to a different equilibrium value.

Figure 2 shows the estimates of η (top plot) and the wind disturbance components (bottom plots) obtained with a single UIO designed as described in Section V, using equations (21) and R computed from (24) and (25) with $\bar{\eta} = 0.1$. We compared two choices for the eigenvalues of F in (21). The thin red lines in Figure 2 correspond to $\lambda_1 = \lambda_4 = 1$, and $\lambda_2 = \lambda_3 = 3000$, that is, 'fast' eigenvalues for the observer components associated with the estimation of the wind disturbances. The thick blue lines correspond to overall 'slow' eigenvalues, $\lambda_1 = \lambda_4 = 1$, $\lambda_2 = \lambda_3 = 10$. For both choices, the estimate of η coincides. The estimate of the wind disturbance components, on the other hand, is reasonably good for the 'fast' observer and considerably deteriorates for the 'slow' observer. This is to be expected due to the high-frequency content of the wind accelerations. We note that the use of a 'fast' observer requires fast measurements (which may be unrealistic without special instruments and processing) and is not needed for the performance of the ice estimation. Indeed, the estimate if η is fairly accurate with the 'slow' observer, with errors that are small around the value $\eta = \bar{\eta} = 0.1$, and larger the farther η is from 0.1.

Next, we design a bank of $N \in [2, 10, 20]$ UIOs as described in Section VI. Figure 3 shows in the top plot the resulting estimate of η obtained with Algorith VI.1. The estimation error for both the single UIO and the bank of UIOs are shown in the bottom plot of Figure 3, where a notable reduction of the error for the UIO bank can be observed. Also note that most of the gain is already obtained for $N = 10$ as the improvement between $N = 10$ and

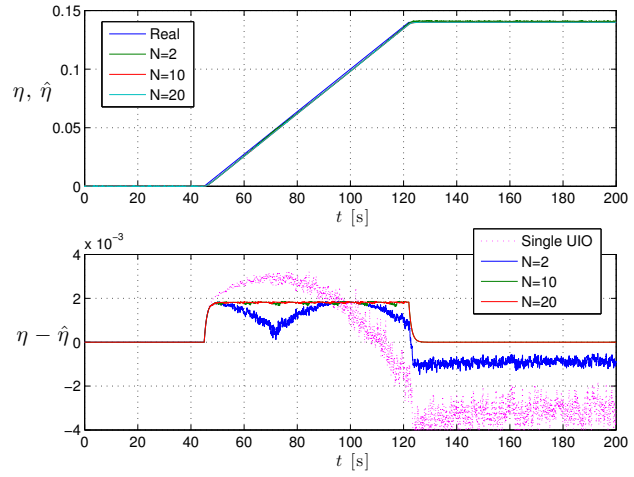

Fig. 3. Estimation of η using a bank of UIOs (top) and estimation error for both the single UIO and the bank of UIOs (bottom), for $N = 3, 10, 20$.

$N = 20$ is only marginal.

As a final test, we considered the more realistic situation of having additive errors/noise in the measurements. Noise with amplitude 0.1 m/s was added to the horizontal and vertical airspeed measurements, whereas for the angle related measurements, slowly varying errors (dominated by bias drift phenomena, as is typically the case for this type of sensors) was considered, with magnitude 0.1 deg for pitch, and 0.01 deg/s for pitch rate. The resulting estimates of η, both for a single UIO and for a bank of $N = 2$ UIOs, and the corresponding estimation errors, are shown in Figure 4. It can be seen that the estimates are still reasonably good although the advantage of using more than one UIO is marginal (tests for $N > 2$ showed no improvement with respect to $N = 2$).

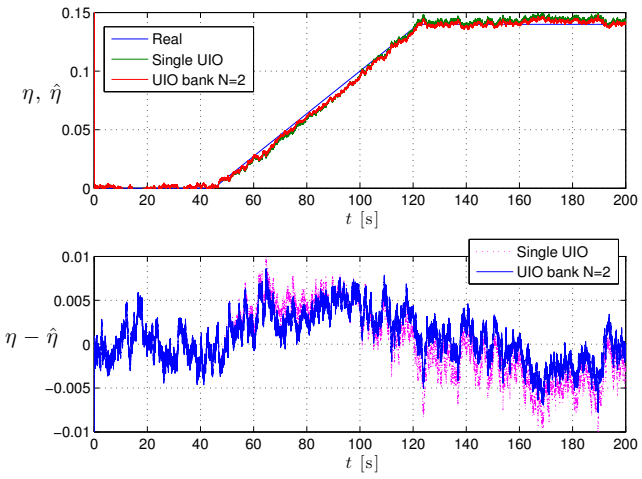

Fig. 4. Estimation of η (top) and estimation error (bottom) under noisy measurements.

VIII. Conclusions

We have considered the problem of detection of icing and estimation of its severity factor in longitudinal control of UAVs. We have proposed to employ a bank of unknown input observers (UIOs), each designed to match a model of the aircraft under a particular level of icing taken from a quantisation of the icing's severity factor range of variation. The UIO design exploits the change in equilibrium conditions, caused by the icing effect, to identify a direction in the observer estimation error space that allows for aircraft icing detection and estimation. By selecting at each time the observer from the bank that yields the smallest value of a suitable residual signal, the icing severity factor can be estimated with an accuracy that is inversely proportional to the size of the quantisation level. Simulation results on a case study of a small UAV have demonstrated the efficiency of the proposed estimation algorithm. Future work will consider the effect of an external control loop that adjusts the operating setpoints and the derivation of bounds on the estimation error guaranteeing a specified accuracy level.

References

[1] R. Beard and T. McLain, *Small unmanned aircrafts – Theory and practice*. Princeton University press, 2012.

[2] S. Bone and M. Duff, "Carbon nanotubes to de-ice UAVs," http://136.142.82.187/eng12/Author/data/2122.docx, Tech. Rep., 2012.

[3] F. Caliskan and C. Hajiyev, "A review of in-flight detection and identification of aircraft icing and reconfigurable control," *Progress in Aerospace Sciences*, vol. 60, pp. 12–34, 2013.

[4] J. Chen, R.Patton, and H.Zhang, "Design of unknown input observers and robust detection filters," *Int. J. of Control*, vol. 63, pp. 85–105, 1996.

[5] A. Cristofaro and T. Johansen, "An unknown input observer approach to icing detection for unmanned aerial vehicles," in *American Control Conference*, Chicago, 2015.

[6] A. Cristofaro, T. Johansen, and A. P. Aguiar, "Icing Detection and Identification for Unmanned Aerial Vehicles: Multiple Model Adaptive Estimation," in *European Control Conference*, Linz, 2015.

[7] R. Gent, N. Dart, and J. Cansdale, "Aircraft icing," *Phil. Trans. of the Royal Soc. of London. Series A: Mathematical, Physical and Engineering Sciences*, vol. 358, pp. 2873–2911, 2000.

[8] H. Haimovich and M. Seron, "Componentwise ultimate bound and invariant set computation for switched linear systems," *Automatica*, vol. 46, no. 11, pp. 1897–1901, 2010.

[9] J. Langelaan, N. Alley, and J. Neidhoefer, "Wind field estimation for small unmanned aerial vehicles," *Journal of Guidance, Control and Dynamics*, vol. 34, no. 4, 2011.

[10] H. Miller and W. Ribbens, "Detection of the loss of elevator effectiveness due to aircraft icing," in *37th AIAA aerospace sciences meeting and exhibit*, Reno,NV, 1999.

[11] D. Pokhariyal, M. Bragg, T. Hutchison, and J. Merret, "Aircraft flight dynamics with simulated ice accretion," in *39th AIAA aerospace sciences meeting and exhibit*, Reno,NV, 2001.

[12] K. Sørensen, M. Blanke, and T. Johansen, "Diagnosis of wing icing through lift and drag coefficient change detection for small unmanned aircraft," in *9th IFAC Symposium on Fault Detection, Supervision and Safety of Technical Processes (SafeProcess 2015)*, Paris, France, September 20155.

[13] M. Tousi and K. Khorasani, "Robust observer-based fault diagnosis for an unmanned aerial vehicle," in *IEEE International Systems Conference (SysCon)*, Montreal, QC, Canada, 2011, pp. 428–434.

[14] A. Varga, *Fault Tolerant Flight Control*. Springer, 2010, ch. Detection and isolation of actuator/surface faults for a large transport aircraft, pp. 423–448.